Iranian Journal of Numerical Analysis and Optimization
Vol. 16, No. 3, 2026, pp 757–789
https://doi.org/10.22067/ijnao.2026.96102.1757
https://ijnao.um.ac.ir/

Research Article

A fitted numerical technique for a class of singularly perturbed delay differential equations

A. Mardi*, H. Shankar Prasad

Abstract

This paper examines the applicability of a new exponentially fitted scheme on Shishkin mesh for solving a class of singularly perturbed problems in ordinary differential equations containing a small delayed term. The original delayed problem is reduced to an equivalent new problem using Taylor series expansion procedure, and then a three-term recurrence relationship is obtained by approximating the first and second-order derivatives in the reduced problem by their mixed and central difference analogue, respectively. To avoid the nonuniformity in the solution, a fitting factor is introduced into the obtained tri-diagonal scheme, and its value is determined by the use of singular perturbation theory. Thomas algorithm is efficiently used to solve a tridiagonal system of equations. Convergence and stability of the scheme are discussed in detail. Richardson's extrapolation technique is employed to improve the accuracy and rate of convergence of the solution produced by the scheme. Four standard example problems are solved, and the computational results are presented in terms of the maximum absolute point-wise errors and rate of convergence. Computational results are compared with some other

*Corresponding author

Received 21 October 2025; revised 3 January 2026; accepted 4 January 2026

Anupam Mardi
Department of Mathematics, National Institute of Technology Jamshedpur, Jharkhand - 831014, India. e-mail: anupammardiapril@gmail.com

Hari Shankar Prasad
Department of Mathematics, National Institute of Technology Jamshedpur, Jharkhand - 831014, India. e-mail: hsprasad.math@nitjsr.ac.in

How to cite this article
Mardi, A. and Shankar Prasad, H., A fitted numerical technique for a class of singularly perturbed delay differential equations. *Iran. J. Numer. Anal. Optim.*, 2026; 16(3): 757-789. https://doi.org/10.22067/ijnao.2026.96102.1757

published results. Theoretical and computational analysis reveal that the fitted scheme is able to produce accurate and uniformly convergent solutions with first-order accuracy, which is further improved to second-order accuracy by Richardson extrapolation. Furthermore, the method is most suitable for all the values of $(1/N) \gg \varepsilon$, where $\varepsilon \leq 10^{-6}$ and N is the number of subintervals in which the underlying interval is divided.

AMS subject classifications (2020): 34D15 · 34E15 · 34E20 · 34B25

Keywords: Singular perturbation problem · Boundary layer · Differential-difference equation · Fitting factor · Thomas Algorithm · Stability and convergence

1 Introduction

It is well known that the singularly perturbed delay differential equations (SPDDEs) or differential-difference equations with interval boundary conditions (IBCs) are the result of mathematical modeling of various physical and biological phenomena/processes/problems. These SPDDEs with IBCs are most ubiquitous and arise in situations in which the future state of the system depends upon the present as well as the past. There are a number of realistic model singularly perturbed problems in differential-difference equations in which one encounters the SPDDEs with IBCs. The first exit time problems in the modeling of activation of neurons and variational problems in control theory are two examples of such problems. The importance of these singularly perturbed problems in differential-difference equations (SPPDDEs) can be easily realized from the research articles and monographs [34, 37, 41, 55, 46, 23, 6, 22, 69, 74, 53, 38, 5, 11, 8, 19, 72, 73, 54, 71]. These SPDDEs are ordinary/partial differential equations in which the highest order derivative is multiplied by a small singular perturbation parameter ε $(0 < \varepsilon \ll 1)$ and the term(s) contain delay (negative shift) and/or advance (positive shift) argument(s). The solution of such problems exhibits oscillatory and/or boundary/interior layer behavior in the underlying interval of interest. In fact, the solution is of multi-scale character when the ε is small tending to zero. That is there exist thin transition layer(s) where the solution undergoes drastic change, while away from the layer(s) the solution behaves regularly and varies slowly. Here, the word “layer” stands for the small subregion of the independent variable over which the dependent variable experiences the most rapid change and the terms boundary and interior layers are due to the occurrence of the layer in the neighborhood of the end and the interior points of the underlying domain, respectively. These thin layers are usually termed as the boundary layers, shock layers, skin layers and transitional points in the various fields of applied science and engineering.

Development of numerical/analytical methods has been a herculean task due to such abnormal layer behavior of solutions. It has been experienced that the error in solving such problems by applying classical numerical methods cannot be reduced below a certain fixed limit unless specially designed numerical methods or nonuniform meshes are used [47]. Thus, the study of such a pervasive problem is vital if robust and accurate solutions are required. More detailed information can be obtained from the monographs: [18, 10, 9, 56, 57, 55, 8] and the research articles: [20, 52, 75, 63, 67, 29, 26, 28, 36, 33, 61, 66, 25, 65, 27, 1, 62, 30, 40, 39, 59, 60, 15, 17, 7, 32, 21, 76].

This paper considers a class of second-order SPDDEs in ordinary differential equations having small delay (δ) in both the convection and reaction terms:

$$\varepsilon y''(s) + b(s)y'(s-\delta) + c(s)y(s-\delta) + d(s)y(s) = f(s) \tag{1}$$

$$\begin{aligned} \text{with the IBCs: } \; & y(s) = \alpha(s) \text{ on } -\delta \leq s \leq 0 \; \text{ and} \\ & y(s) = \beta(s) \text{ on } 1 \leq s \leq 1+\delta, \end{aligned} \tag{2}$$

where the functions $b(s)$, $c(s)$, $d(s)$, and $f(s)$ are sufficiently continuously differentiable functions over $[0,1]$ with $b(s) \geq b_* > 0$; α and β are considered to be constants.

The solution of SPDDE (1) with the IBCs (2) exhibits boundary layer behavior at left-end of the interval $[0,1]$ when $b(s) - \delta c(s) \geq M > 0$, where M is considered to be a positive real number. When $b(s) - \delta c(s) \leq M < 0$, the solution exhibits boundary layer at the right-end of the underlying domain.

Such SPPDDEs have grabbed a great deal of attention in the recent and past years. In a series of papers, [38, 39, 40, 42, 41], Lange and Miura performed the singular perturbation analysis of boundary-value problem for differential-difference equations with small shifts. In the papers [41] and [42], they employed asymptotic approaches to approximate the solution of BVPs for the two classes of singularly perturbed problems in differential-difference equations with small shifts. In the article [42], they studied the effect of small shifts on the oscillatory behavior of the solution and remarked that the shifts affect oscillatory solutions more than the boundary layer solutions. They pointed out that the delayed term can be approximated by the use of the Taylor series expansion procedure in the case when the delay is of a small order of ε [42]. There are many references in the literature where the shifts are very small and affect the solution considerably. Lange and Miura [42] have demonstrated that the effect of very small shifts on the solution behavior by considering several numerical example problems in which the shifts are of small order of ε. They pointed out that the small shifts affect the solution considerably and cannot be neglected. The biologist Hutchinson [24] also found that “there is a tendency for the time lag to be reduced as much as possible by natural selection". The arguments for small delay problems are found throughout the literature on epidemics and populations. Thus the small shifts play an important role in practical problems [34]. In the article [35] the authors have devised a B-spline based numerical method to treat singular perturbation problems (SPPs) having delays in the convection and reaction term over a piece-wise uniform mesh. The convergence of the method is thoroughly discussed. The method is achieving almost second-order convergence. In the article [77], the authors have suggested an exponentially fitted mid-point upwind finite difference method for solving a class of convection-diffusion SPDDEs. The proposed method achieves linear order convergence. A nonsymmetric finite difference based scheme has been devised by the authors in the article [78] to treat convection type SPPs having delay shift. The terms containing the delay parameter are expanded up-to second-order using the well-known Taylor series expansion. Theoretical and numerical examinations reveal that the method is achieving second-order convergence. Authors in [58] have carried out a numerical integration technique to treat a class of SPDDEs which yields a tri-diagonal system that has been solved by Thomas algorithm. This scheme has been performed on some example problems to validate the scheme. A detailed discussion has been done on how the change of the shift parameter affects the layer behavior of the solution. The author in [60] has developed a cubic spline-based numerical solving technique for SPDDEs having delays in the convection and reaction terms. The computational results have been compared with some published results. The author has observed that the scheme achieved second-order rate of convergence (ROC) as $\varepsilon \geq h$ but losses an order when $\varepsilon \ll h$ and tending to zero. Similar types of problems are discussed in the paper [3]. Here, the authors have proposed a central finite difference based exponentially fitted scheme for solving it using uniform mesh discretization. The numerical and experimental analysis reveals that the method is of quadratic order convergence for $\varepsilon = O(N^{-1})$. On the other hand, the method achieves linear order convergence for $\varepsilon \ll N^{-1}$ which indicates the fact that the ROC of the method is ε-dependent. The depicted figures for the solution to the example problems, show that the width of the boundary layer decreases as the perturbation parameter goes smaller.

In this article, we have proposed a novel exponentially fitted scheme for numerical solution of SPDDE (1) with the IBCs (2). The negative shift (or delay parameter) induces memory effect into the problem, that is the solution of the problem at any moment depends upon the solution of the problem at some earlier moment. Taylor's series expansion is used to approximate the delayed terms and the first- and second-order derivatives in the reduced equivalent problem are approximated by the first-order mixed finite differences and second-order central differences respectively, which leads to generating a tridiagonal system of equations. Application of Taylor series expansion is justified due to the reason that the delay δ is of a small order of ε. A suitable fitting factor that involves the exponential function has been introduced into the scheme to avoid the nonuniformity in the solution. The resulting system is solved by "Discrete Invariant Imbedding Algorithm" widely known as "Thomas Algorithm". To improve the accuracy of the solution produced by the proposed scheme and ROC of the scheme, we have applied Richardson extrapolation procedure to it. The stability and convergence of the fitted scheme have been discussed in detail. To confirm the applicability of the proposed scheme, four example problems have been solved for diverse values of δ and ε. The computational results are tabulated in terms of maximum absolute point-wise errors (MAPEs) and the ROCs before and after applying Richardson extrapolation. Numerical experiments show that the scheme is capable of producing better results than the results obtained in [60, 3, 58, 41]. For more clarity, the solutions of the problems have been plotted graphically for different values of ε, N, and δ, which reveals that as δ increases and $\varepsilon \to 0$ the thickness of the boundary layer decreases. Also, the log-log plot of MAPEs vs N for the problems have also been done which shows the relation between the ε, N, and MAPEs.

Here, the novelty of the proposed method is associated with the improvement in the accuracy of the solutions obtained and the ROC achieved, when the Richardson extrapolation procedure is applied. There are some methods/ schemes for which the accuracy of the solutions obtained improves but the ROC does not improve when the Richardson extrapolation procedure is applied on it. In the articles [50, 51], the authors have shown that the Richardson extrapolation does not improve the ROC of the method while there is an improvement in the accuracy of the solutions. Nevertheless, in the case of the proposed scheme, an application of the Richardson extrapolation noticeably improves the accuracy as well as the ROC. This fact strengthens the claim "A numerical solution of required accuracy can be obtained by using Richardson extrapolation" [2, 68]. Furthermore, from the point of view of the wealth of the literature on singular perturbation problems, we always raise a question that whether there are other ways to deal with the SPPs which can be used easily with minimal amount of computational work (problem preparation). Motivated from this question, we have successfully devised a new exponentially fitted finite difference method for solving the considered SPPDDEs. Method is capable of producing highly accurate and uniformly convergent results with quadratic ROC for all the values of $(1/N) \gg \varepsilon$, where $\varepsilon \leq 10^{-6}$ and N is the number of subintervals in which the underlying interval is divided. Furthermore, our method does not depend upon any other parameters as used in [31, 64]

The remaining part of the article has been arranged in the following manner:
In Section 2, an approximated version of the original problem is deduced by the use of Taylor series; In Section 3, Shishkin mesh is described. In Section 4, we have derived the proposed scheme. In Section 5, stability of the proposed method is thoroughly discussed. In Section 6, Richardson's extrapolation procedure is discussed in detail. In Section 7, we have applied the proposed method to some example problems to establish the applicability of the method. The

results produced by the method are presented in tabular form. In Section 8, we have summarized the paper work. Paper ends with the references.

2 Approximate problem and solution properties

Using the Taylor series, we have

$$\left.\begin{aligned} y(s-\delta) &\quad \approx y(s) - \delta\, y'(s) + \mathcal{O}(\delta^2), \\ y'(s-\delta) &\quad \approx y'(s) - \delta\, y''(s) + \mathcal{O}(\delta^2). \end{aligned}\right\} \tag{3}$$

Using the above expansions into (1), we get

$$\mu y''(s) + p(s)y'(s) + q(s)y(s) = f(s), \quad s \in [0,1], \tag{4}$$

with

$$y(0) \approx \alpha(0) \;\text{ and }\; y(1) \approx \beta(1). \tag{5}$$

where $\mu = \varepsilon - \delta b(s)$, $p(s) = b(s) - \delta c(s)$ and $q(s) = c(s) + d(s)$, respectively, and it is presumed that $q(s) \leq 0$.

The SPDDE (4)–(5) is different from the original problem (1)–(2) by the term $(\mathcal{O}(\delta^2)y'' + \mathcal{O}(\delta^2)y''')$, which is a good approximation of the original problem. The use of Taylor's series expansion in approximating the term containing delay arguments (δ) is valid because of the fact that the values of delay δ are considered to be of $o(\varepsilon)$ [42, 41].

As the new equivalent version of the original problem (4)–(5) differs from the original problem (1)–(2) by the term $(\mathcal{O}(\delta^2)y'' + \mathcal{O}(\delta^2)y''')$, we prefer a new notation say $\lambda(s)$ for the solution of the approximated version of (1)–(2). Thus (4)–(5) can be written as

$$\mathcal{L}\lambda := \mu\lambda''(s) + p(s)\lambda'(s) + q(s)\lambda(s) = f(s), \quad s \in [0,1], \tag{6}$$

with

$$\lambda(0) = \alpha(0) = \alpha_0 \;\text{ and }\; \lambda(1) = \beta(1) = \beta_1. \tag{7}$$

The solution of the problem (6)–(7) can be decomposed as

$$\lambda = v + w. \tag{8}$$

For any $k_1 > 0$, the regular part v satisfies

$$|v^{(k)}(s)| \leq C \quad \text{for} \quad k = 0, 1, \ldots, k_1, \tag{9}$$

and the layer part w satisfies

$$|w^{(k)}(s)| \leq C\mu^{-k} e^{-p_*(1-s)/\mu} \quad \text{for} \quad k = 0, 1, \ldots, k_1. \tag{10}$$

Furthermore, we have

$$\mathcal{L}v = f \quad \text{and} \quad \mathcal{L}w = 0; \tag{11}$$

see [44].

3 Description of the Shishkin-mesh

In order to obtain the discretized scheme on the Shishkin mesh, we divide the considered interval, $[0, 1]$ into N subintervals such that $X_N = \{0 = s_1 < s_2 < s_3 < \cdots < s_N < s_{N+1} = 1\}$, where N is the multiple of 2. Now, we divide the interval $[0, 1]$ into two subintervals $[0, \tau]$ and $[\tau, 1]$, where the transition parameter τ is given by

$$\tau = \min\left(\frac{1}{2}, \frac{2\mu}{p^*}\ln(N)\right),$$

where p^* is the maximum value of p over $[0, 1]$. The mesh points are given by

$$\begin{aligned} s_{i+1} &= \frac{i}{N/2}\tau, \quad i = 0, 1, 2, \ldots, \frac{N}{2}, \\ s_{\frac{N}{2}+i+1} &= \tau + \frac{i}{N/2}(1-\tau), \quad i = 1, 2, \ldots, \frac{N}{2}, \end{aligned} \tag{12}$$

where the step lengths $h_i = s_{i+1} - s_i \quad i = 1, 2, 3, \ldots, N$ and $h = \max\{h_i\}, \quad i = 1, 2, 3, \ldots, N$. Let the function ϕ denote the mesh generating function over the interval $[0, s_{(N/2)+1}]$ and defined in such a way that $\phi(0) = 0$ and $\phi(\frac{1}{2}) = \frac{\ln(N)}{p^*}$, where ϕ is a continuously differentiable monotonically increasing function. We define another function ψ such that

$$\phi = -\ln\psi. \tag{13}$$

This function is monotonically decreasing with $\psi(0) = 1$ and $\psi(1/2) = e^{-\frac{lnN}{p^*}}$, which gives

$$\psi(s) = e^{-2\frac{(\ln N)s}{p^*}}. \tag{14}$$

4 Description of the proposed scheme

In this section, we will discuss the proposed scheme step by step for obtaining the solution of the problem (6)–(7).

By the theory of singular perturbation, the solution of the problem (6)–(7) can be written as (see . 22–261[56])

$$\lambda(s_i) = \lambda_0(s_i) + (\alpha - \lambda_0(0)) \exp\Big(- \Big(\frac{p(0)}{\mu} - \frac{q(0)}{p(0)}\Big)\Big). \tag{15}$$

Taking $h_i \to 0$ and using (15), we get

$$\lim_{h\to 0} \lambda_i = \lim_{h_i\to 0} \lambda(s_i) = \lambda_0(0) + (\alpha - \lambda_0(0)) \exp\Big(- \Big(\frac{p^2(0) - \mu q(0)}{p(0)}\Big) i\rho\Big), \tag{16}$$

where $\rho = \frac{h}{\mu}$ is called "density factor".

Approximating the first-order derivative and using the mixed finite difference analogue,

$$\lambda'_i = \alpha\left(\frac{\lambda_{i+1}}{2h_i} - \frac{\lambda_{i-1}}{2h_i}\right) + (1-\alpha)\left(\frac{\lambda_{i+1}}{h_i} - \frac{\lambda_i}{h_i}\right) + \mathcal{O}(h_i) \quad \text{with} \quad \alpha = \frac{1}{2};$$

that is,

$$\lambda'_i = \frac{3\lambda_{i+1} - 2\lambda_i - \lambda_{i-1}}{4h_i}, \tag{17}$$

and the second-order derivative by the second-order central difference

$$\lambda''_i = \frac{\lambda_{i+1} - 2\lambda_i + \lambda_{i-1}}{{h_i}^2}, \tag{18}$$

we obtain

$$\mu\Big[\frac{\lambda_{i+1}}{{h_i}^2} - \frac{2\lambda_i}{{h_i}^2} + \frac{\lambda_{i-1}}{{h_i}^2}\Big] + p_i\Big[\frac{3\lambda_{i+1}}{4h_i} - \frac{2\lambda_i}{4h_i} - \frac{\lambda_{i-1}}{4h_i}\Big] + q_i\lambda_i = f_i. \tag{19}$$

Introducing a fitting factor $\sigma(\rho)$ into (19), we get

$$\sigma(\rho)\mu\Big[\frac{\lambda_{i+1}}{{h_i}^2} - \frac{2\lambda_i}{{h_i}^2} + \frac{\lambda_{i-1}}{{h_i}^2}\Big] + p_i\Big[\frac{3\lambda_{i+1}}{4h_i} - \frac{2\lambda_i}{4h_i} - \frac{\lambda_{i-1}}{4h_i}\Big] + q_i\lambda_i = f_i. \tag{20}$$

Multiplying (19) by h_i and taking $h_i \to 0$, we get

$$\frac{\sigma(\rho)}{\rho}\Big[\lambda_{i+1}-2\lambda_i+\lambda_{i-1}\Big]+p_i\Big[3\lambda_{i+1}-2\lambda_i-\lambda_{i-1}\Big]=0. \tag{21}$$

Using (16), we get

$$\lim_{h_i\to 0}(\lambda_{i+1}-2\lambda_i+\lambda_{i-1})=(\alpha-\lambda_0(0))e^{-i\kappa\rho}\big(e^{\kappa\rho}+e^{-\kappa\rho}-2\big),$$

$$\lim_{h_i\to 0}(3\lambda_{i+1}-2\lambda_i+\lambda_{i-1})=(\alpha-\lambda_0(0))e^{-i\kappa\rho}\big(3e^{-\kappa\rho}-e^{\kappa\rho}-2\big),$$

where $\kappa=\frac{p^2(0)-\mu q(0)}{p(0)}$.

By using the above two equations, the fitting factor is obtained as follows:

$$\begin{aligned}\sigma(\rho)&=\frac{p(0)\rho}{2}\cdot\frac{e^{\frac{k\rho}{2}}-e^{\frac{-k\rho}{2}}}{e^{\frac{k\rho}{2}}+e^{\frac{-k\rho}{2}}}-\frac{p(0)\rho}{4}\\&=\frac{p(0)\rho}{2}\coth\left(\frac{p^2(0)-\mu q(0)}{p(0)}\frac{\rho}{2}\right)-\frac{p(0)\rho}{4}.\end{aligned} \tag{22}$$

Finally, (20) gives the recurrence relation as follows:

$$\mathcal{E}_i\lambda_{i-1}-\mathcal{F}_i\lambda_i+\mathcal{G}_i\lambda_{i+1}=\mathcal{H}_i,\qquad i=2,\dots,N, \tag{23}$$

where

$$\begin{aligned}\mathcal{E}_i&=\frac{\sigma\mu}{{h_i}^2}-\frac{p_i}{4h_i},\\\mathcal{F}_i&=\frac{2\sigma\mu}{{h_i}^2}+\frac{2p_i}{4h_i}-q_i,\\\mathcal{G}_i&=\frac{\sigma\mu}{{h_i}^2}+\frac{3p_i}{4h_i},\\\mathcal{H}_i&=f_i.\end{aligned}$$

Equation (23) with boundary conditions (7) generates $(N-1)\times(N-1)$ system of equations. This system is solved by the Thomas Algorithm. The stability conditions for the algorithm are $\mathcal{E}_i>0$, $\mathcal{F}_i>0$ and $\mathcal{G}_i>0$, $\mathcal{E}_i+\mathcal{G}_i\geq\mathcal{F}_i$. In this method, if $q(s)\leq 0$ holds, then one can easily show the stability of the algorithm.

5 Stability analysis

5.1 Consistency

Let us consider

$$\bar{\tau}_i[\lambda_i] \equiv \mathcal{L}_{h_i}\lambda(s_i) - \mathcal{L}\lambda(s_i), \quad i = 1, 2, \cdots, N+1,$$

where λ is a smooth function over $\mathcal{I} = [0, 1]$ with $\mathcal{L}_{h_i}$ as the finite difference operator. Then the problem finite difference problem (23)–(7) is consistent with the differential problem (6)–(7) if

$$|\bar{\tau}_i[\lambda]| \to 0 \quad \text{when} \quad h \to 0,$$

where $\bar{\tau}_i[\lambda], \quad i = 1, \ldots, N+1$ are the local truncation errors.

5.2 Accuracy

The solution of the problem (6)–(7) is said to be accurate of order p if for a positive constant $\mathcal{C}$ independent of h and μ, there exists a relation of the form:

$$|\bar{\tau}_i[\lambda]| \le \mathcal{C}h^p, \quad i = 1, 2, \cdots, N+1.$$

Assumption 1. Throughout the paper, we shall assume that

$$\mu \le \mathcal{C}N^{-1}, \tag{24}$$

which is generally in the case for discretization of the convection-dominated problems.
Assumption 2. $\mathcal{L}^N$ follows the bound

$$|\mathcal{L}^N\lambda(s_i) - \mathcal{L}\lambda(s_i)| \le 2\mu \int_{x_{i-1}}^{s_{i+1}} |g'''(s)|ds + q_i \int_{s_i}^{s_{i+1}} |g''(s)|ds, \tag{25}$$

where g is any function $g \in C^3[0, 1]$.

Lemma 1 (Kellogg and Tran)**.** If $b(s)$, $c(s)$, $d(s)$ are sufficiently smooth and independent of μ, then the the solution $\lambda(s)$ satisfies the inequality,

$$|\lambda^{(k)}(s)| \le \mathcal{C}\big(1 + (\varepsilon - \delta b_*)^{-k} e^{\frac{-M's}{(\varepsilon-\delta b_*)}}\big), \quad k = 0, 1, 2, \ldots. \tag{26}$$

Proof. See [48]. □

Theorem 1. Let us consider that the piece-wise differentiable mesh generating function ψ satisfies the condition

$$\frac{\max \phi'}{N} \leq \mathcal{C} \tag{27}$$

and

$$\int_0^{\frac{1}{2}} \phi'(x)^2 dx \leq \mathcal{C}N. \tag{28}$$

Then the error of the scheme (17) satisfies

$$|\lambda(s_i) - \lambda_N(s_i)| \leq, \begin{cases} \mathcal{C}N^{-1} \max|\psi'|, & \text{for } i = 1, \dots, N/2, \\ \mathcal{C}N^{-1}, & \text{for } i = (N/2)+1, \dots, N+1. \end{cases} \tag{29}$$

Proof. The mesh size h_i on the fine mesh satisfies

$$h_i = 2\mu\big(\psi(s_i) - \psi(s_{i-1})\big) \leq 2\mu N^{-1} \max \psi' \quad \text{for} \quad i = 2, \dots, (N/2)+1. \tag{30}$$

Thus

$$h_i \leq \mathcal{C}N^{-1}, \quad \text{for} \quad i = 2, \dots, N+1, \tag{31}$$

by using (14) and the Assumption 1 and (27).

Now, using the decomposition in [44] of λ, we split the solution of the discrete problem as

$$\mathcal{L}^N v_i^N = f_i \quad \text{for} \quad i = 2, \dots, N+1, \quad \text{for} \quad v_1^N = v_1, \quad v_{N+1}^N = v_{N+1}$$

and

$$\mathcal{L}^N w_i^N = 0 \quad \text{for} \quad i = 2, \dots, N+1, \quad \text{for} \quad w_1^N = w_1, \quad w_{N+1}^N = w_{N+1}.$$

□

An immediate consequence of (9), (25), M-matrix property of $\mathcal{L}^N$, and (31),

$$|v_i - v_i^N| \leq \mathcal{C}N^{-1} \qquad \text{for} \quad i = 1, \dots, N+1. \tag{32}$$

Using the M-matrix property of $\mathcal{L}^N$, one can show that

$$w_i^N \leq \prod_{k=2}^{(N/2)+1} \left(1 + \frac{h_k}{2\mu}\right)^{-1}, \quad \text{for } i = (N/2)+1, \dots, N+1, \tag{33}$$

from [43, 45, 70]. We have

$$\ln\left(\prod_{k=2}^{(N/2)+1}\left(1+\frac{h_k}{2\mu}\right)\right) \geq \sum_{k=2}^{(N/2)+1}\left(\frac{h_k}{2\mu}-\frac{1}{2}\left(\frac{h_k}{2\mu}\right)^2\right)$$
$$\geq \ln N - \frac{1}{2}\sum_{k=2}^{(N/2)+1}\left(\frac{h_k}{2\mu}\right)^2.$$

Therefore,

$$\prod_{k=2}^{(N/2)+1}\left(1+\frac{h_k}{2\mu}\right)^{-1} \leq N^{-1}\exp\left(\frac{1}{2}\sum_{k=2}^{(N/2)+1}\left(\frac{h_k}{2\mu}\right)^2\right).$$

Now, the representation

$$\frac{h_k}{2\mu} = \int_{s_{k-1}}^{s_k}\phi'(x)\,dx, \quad \text{for } k=2,\dots,(N/2)+1,$$

yields

$$\sum_{k=2}^{(N/2)+1}\left(\frac{h_k}{2\mu}\right)^2 \leq \sum_{k=2}^{(N/2)+1}(s_k-s_{k-1})\int_{s_{k-1}}^{s_k}\phi'(x)^2\,dx = N^{-1}\int_0^{1/2}\phi'(x)^2\,dx.$$

Thus, if assumption (28) holds true, then (33) yields

$$w_i^N \leq \mathcal{C}N^{-1} \quad \text{for } i=(N/2)+1,\dots,N+1.$$

Consequently,

$$|w_i - w_i^N| \leq |w_i| + |w_i^N| \leq \mathcal{C}N^{-1} \quad \text{for } i=(N/2)+1,\dots,N+1. \tag{34}$$

For the truncation error of the method with respect to the layer part w, inequalities (10) and (25) imply that

$$\bar{\tau}_i := \|\mathcal{L}^N[w_i - w_i^N]\| \leq \mathcal{C}\mu^{-2}\int_{x_{i-1}}^{x_{i+1}} e^{-p_*(1-s)/\mu}\,dx \quad \text{for } i=2,\dots,N.$$

Substituting $x = 2\mu\phi(s)$ on the fine part of the mesh, we obtain

$$\bar{\tau}_i \leq \mathcal{C}(e^{p_*/\mu})\mu^{-1}\int_{s_{i-1}}^{s_{i+1}} e^{-2\phi(s)}\phi'(s)\,ds = \mathcal{C}(e^{p_*/\mu})\mu^{-1}\int_{s_{i-1}}^{s_{i+1}} e^{-\phi(s)}|\psi'(s)|\,ds$$

for $i=2,\dots,N/2$. Let $s \in [s_{i-1}, s_{i+1}]$ be arbitrary. Then we have

$$e^{-\phi(s)} \leq e^{-s_{i-1}/(2\mu)} = e^{-s_i/(2\mu)} e^{(x_i - s_{i-1})/(2\mu)} = e^{-s_i/(2\mu)} e^{h_i/(2\mu)} \leq \mathcal{C} e^{-s_i/(2\mu)},$$

by (27) and (30). Thus

$$\bar{\tau}_i \leq \mathcal{C}(e^{p_*/\mu})\mu^{-1} N^{-1} e^{-s_i/(2\mu)} \max|\psi'| \quad \text{for } i = 2, \ldots, N/2.$$

Now, the discrete comparison principle based on the barrier function presented in [70] (see also [43, 45]) yields

$$|E_i - E_i^N| \leq \mathcal{C} N^{-1} \max|\psi'| \quad \text{for } i = 2, \ldots, (N/2) + 1. \tag{35}$$

Combining (32), (34), and (35), we are done.

This shows that the proposed new scheme is linearly convergent.

Now, the Richardson extrapolation technique is described for improving the accuracy and ROC of the solution obtained by the proposed scheme (23).

6 Richardson extrapolation

It is well known that the Richardson extrapolation procedure is designed to enhance the ROC of the scheme/method and the accuracy of the computed solutions. This procedure can be described as follows:

Let $X_N \subset X_{2N}$, where X_{2N} is the set of mesh points obtained by bisecting the step size of X_N. Let $\lambda_{2N}(s)$ be the solution obtained for X_{2N}. Let $\lambda_N(s_i)$ be the numerical solution of the fully discretized scheme (23) over X_N. Then using (29) of Theorem 1, one can write

$$\lambda(s_i) - \lambda_N(s_i) = \mathcal{C}(N^{-1}) + R_N, \quad s_i \in X_N. \tag{36}$$

Similarly, by assuming $\lambda_{2N}(s_i)$ as the numerical solution of the fully discretized scheme equation (23) on X_{2N}, we have

$$\lambda(s_i) - \lambda_{2N}(s_i) = \mathcal{C}\left((2N)^{-1}\right) + R_{2N}, \quad s_i \in X_{2N}. \tag{37}$$

The two remainders R_N and R_{2N} are $\mathcal{O}(N^{-2})$. From (36)–(37), using the approaches in [15, 16, 14], we get

$$\lambda(s_i) - \big(2\lambda_{2N}(s_i) - \lambda_N(s_i)\big) \leq \mathcal{C}\big(N^{-2}\big), \quad s_i \in X_{2N}. \tag{38}$$

Now, we define the extrapolation formula as

$$\lambda_N^{ext}(s) = 2\lambda_{2N}(s) - \lambda_N(s), \tag{39}$$

which gives a better approximation of $\lambda(s_i)$ than either $\lambda_N(s_i)$ or $\lambda_{2N}(s_i)$. The truncation error of spatial discretization after applying the extrapolation to the solution can be written as follows:

$$\begin{aligned}\lambda(s_i) - \lambda^{\text{ext}}(s_i) &= \lambda(s_i) - \big(2\lambda_{2N}(s_i) - \lambda_N(s_i)\big),\\ &= 2\big(\lambda(s_i) - \lambda_{2N}(s_i)\big) - \big(\lambda(s_i) - \lambda_N(s_i)\big), \quad (s_i) \in X_{2N}.\end{aligned} \tag{40}$$

Theorem 2 (Error estimation after applying Richardson extrapolation to the scheme)**.** Let $\lambda(s_i)$ be the solution of (6)–(7) and let $\lambda_N^{\text{ext}}(s_i)$ be the extrapolated solution as defined in 39). Then

$$|\lambda(s_i) - \lambda_N^{\text{ext}}(s_i)| \le \mathcal{C}\big(N^{-2}\big), \quad i = 1, \dots, N+1.$$

Proof. Like the solution $\lambda(s_i)$ of (6)–(7) and the numerical solution $\lambda_N(s_i)$ of (23) in X_N, the numerical solution $\lambda_{2N}(s_i)$ of (23) on X_{2N} can be decomposed into regular $V_{2N}(s_i)$ and singular $W_{2N}(s_i)$ components such that

$$\lambda_{2N}(s_i) = V_{2N}(s_i) + W_{2N}(s_i). \tag{41}$$

Therefore, we have

$$\lambda(s_i) - \lambda_k(s_i) = \begin{cases} v(s_i) - V_{2N}(s_i) + w(s_i) - W_{2N}(s_i), & \text{if } k = 2N,\\ v(s_i) - V_N(s_i) + w(s_i) - W_N(s_i), & \text{if } k = N. \end{cases} \tag{42}$$

The combination of (40) and (42) gives

$$\begin{aligned}\lambda(s_i) - \lambda_N^{\text{ext}}(s_i) &= 2\big(v(s_i) - V_{2N}(s_i)\big) - \big(v(s_i) - V_N(s_i)\big)\\ &\quad + 2\big(w(s_i) - W_{2N}(s_i)\big) - \big(w(s_i) - W_N(s_i)\big)\\ &= v(s_i) - V_N^{\text{ext}}(s_i) + w(s_i) - W_N^{\text{ext}}(s_i),\end{aligned} \tag{43}$$

where $V_N^{\text{ext}}(s_i)$ is the regular component, and $W_N^{\text{ext}}(s_i)$ is the singular component such that $\lambda_N^{\text{ext}}(s_i) = V_N^{\text{ext}}(s_i) + W_N^{\text{ext}}(s_i)$. From (29) and the techniques used in [12, 4] on X_{2N}, we have

$$v(s_i) - V_{2N}(s_i) = \begin{cases} \mathcal{C}\left((2N)^{-1}\right) + (R_1)_{2N}, & 2 \le i \le \dfrac{N}{2} + 1,\\ \mathcal{C}\left((2N)^{-1}\right) + (R_2)_{2N}, & \dfrac{N}{2} + 2 \le i \le N, \end{cases} \tag{44}$$

where $(R_1)_{2N}$ and $(R_2)_{2N}$ are of $\mathcal{O}((h_i/2)^2)$. For $1 \leq j \leq \frac{N}{2}$, by using (29) and (44), we have

$$\begin{aligned} 2\big(v(s_i) - V_{2N}(s_i)\big) - \big(v(s_i) - V_N(s_i)\big) &= \mathcal{C}\left((2N)^{-1}\right) + \mathcal{O}\big((N^{-1})^2\big) - C\left(N^{-1}\right) + \mathcal{O}\big((N^{-1})^2\big) \\ &= \mathcal{O}\big(N^{-2}\big). \end{aligned}$$

Thus,

$$v(s_i) - V_N^{\text{ext}}(s_i) = \mathcal{O}\big(N^{-2}\big). \tag{45}$$

For $\frac{N}{2} + 2 \leq i \leq N$, using the same procedure employed above, we can get the same result (45). Now, consider the singular components in the outer layer region and interior layer region.

First, consider the estimate in the outer layer region $[0, 1-\tau]$. From (10), we have

$$\begin{aligned} |w(s_i)| &\leq \mathcal{C}\exp\left(-\frac{p_*(1-s_i)}{\mu}\right) \leq \mathcal{C}\exp\left(-\frac{p_*(1-(1-\tau))}{\mu}\right) \\ &= \mathcal{C}\exp\left(-\frac{p_*\tau}{\mu}\right) \leq \mathcal{C}N^{-2}, \quad \text{since we assumed } \tau = \frac{2\mu}{p^*}\ln N. \end{aligned} \tag{46}$$

For the solution of the given problem, we consider the following barrier function in order to determine the bound of $|W(s_i)|$:

$$\mathcal{S}(s_i) = \mathcal{C}\prod_{r=1}^{i}\left(1 + \frac{p_* h_r}{\mu}\right)\left[\prod_{r=1}^{N}\left(1 + \frac{p_* h_r}{\mu}\right)^{-1}\right]. \tag{47}$$

By the same technique used in [70], we obtain $|W_N(s_i)| \leq \mathcal{C}N^{-2}$. Therefore,

$$|w(s_i) - W(s_i)| \leq \mathcal{C}N^{-2}. \tag{48}$$

In a similar approach, we can get

$$|w(s_i) - W_{2N}(s_i)| \leq \mathcal{C}N^{-2}. \tag{49}$$

From (48)–(49) for the outer layer region, we obtain

$$|w(s_i) - W_N^{\text{ext}}(s_i)| \leq \mathcal{C}N^{-2}. \tag{50}$$

For the interior layer region $[1-\tau, 1]$, by following the same procedure in

[49, 4, 13], we obtain

$$w(s_i) - W_k(s_i) = \begin{cases} \mathcal{O}\big(N^{-2}\big), & \text{if } k = 2N, \\ \\ \mathcal{O}\big(N^{-2}\big), & \text{if } k = N. \end{cases} \tag{51}$$

Therefore, for the inner layer region, we get

$$|w(s_i) - W_N^{\text{ext}}(s_i)| \leq \mathcal{C}N^{-2}. \tag{52}$$

Hence, the combination of (45), (50), and (52) gives the required result.

□

7 Numerical experiments

To establish the applicability of the proposed numerical scheme, we applied the scheme to some widely discussed example problems and presented the computational results in tabular form in terms of MAPEs and ROCs for diverse values of N and ε. Since the exact solutions of the problems are unknown, "double-mesh principle" [18] is used to compute the MAPEs and ROCs. Thereafter, to increase the accuracy of the solutions and the ROC of the scheme, we applied the Richardson extrapolation technique to it. We calculated the MAPEs (E_ε^N) by the double-mesh principle formula: $E_\varepsilon^N = \max_{1\leq i\leq N+1} |(\lambda_N^{ext})_i - (\lambda_{2N}^{ext})_{2i-1}|$ and the ROCs (R_ε^N) by the formula, $R_\varepsilon^N = \log_2 \frac{E_\varepsilon^N}{E_\varepsilon^{2N}}$.

Problem 1. First, consider the SPDDE with variable coefficient exhibiting left-end boundary layer [60, 3]:
$\varepsilon\lambda''(s) + (1+s)\lambda'(s-\delta) + e^{-2s}\lambda(s-\delta) - 2e^{-s}\lambda(s) = 0$ over [0,1];
with $\lambda(0) = 0$ and $\lambda(1) = 1$.

Problem 2. Now, consider the SPDDE with variable co-efficient exhibiting left-end boundary layer [60]:
$\varepsilon\lambda''(s) + (1+s)\lambda'(s-\delta) + \sin(2s)\lambda(s-\delta) - e^{-s}\lambda(s) = \sin(2s) + 3e^{-s}$ over [0,1];
with $\lambda(0) = 0$ and $\lambda(1) = 1$.

Problem 3. Now, consider the SPDDE with variable co-efficient exhibiting left-end boundary layer [60, 3, 41, 58]:
$\varepsilon\lambda''(x) + e^{s}\lambda'(s-\delta) + s\lambda(s) = 0$ over [0,1];
with $\lambda(0) = 0$ and $\lambda(1) = 1$.

Problem 4. Finally, consider the nonlinear SPDDE with constant co-efficient exhibiting boundary layer at the left-end of the underlying domain [41, 58]:
$\varepsilon\lambda''(s) + \lambda(s)\lambda'(s-\delta) - \lambda(s) = 0$ over [0,1];
with $\lambda(s) = 1, -\delta \leq s \leq 0$, and $\lambda(1) = 1$.

The linear form of the problem:
$\varepsilon\lambda''(s) + \lambda'(s-\delta) - \lambda(s) = 0$ over [0,1];
with $\lambda(0) = 1$ and $\lambda(1) = 1$.

Table 1: MAPEs (E_ε^N) and ROCs (R_ε^N) for diverse values of N and ε of Problem 1 for $\delta = 0.5\varepsilon$

ε	$N=2^3$	$N=2^4$	$N=2^5$	$N=2^6$	$N=2^7$	$N=2^8$	$N=2^9$
before extrapolation							
10^{-6}	8.7523(-003)	4.5022(-003)	2.2956(-003)	1.1627(-003)	5.8468(-004)	2.9337(-004)	1.4705(-004)
R_ε^N	0.9590	0.9718	0.9814	0.9918	0.9949	0.9964	
10^{-7}	8.7520(-003)	4.5019(-003)	2.2953(-003)	1.1625(-003)	5.8439(-004)	2.9307(-004)	1.4715(-004)
R_ε^N	0.9591	0.9719	0.9815	0.9922	0.9957	0.9940	
10^{-8}	8.7520(-003)	4.5019(-003)	2.2952(-003)	1.1624(-003)	5.8436(-004)	2.9305(-004)	1.4718(-004)
R_ε^N	0.9591	0.9719	0.9815	0.9922	0.9957	0.9936	
10^{-9}	8.7520(-003)	4.5019(-003)	2.2952(-003)	1.1624(-003)	5.8436(-004)	2.9304(-004)	1.4719(-004)
R_ε^N	0.9591	0.9719	0.9815	0.9922	0.9958	0.9934	
10^{-10}	8.7520(-003)	4.5019(-003)	2.2952(-003)	1.1624(-003)	5.8436(-004)	2.9305(-004)	1.4718(-004)
R_ε^N	0.9591	0.9719	0.9815	0.9922	0.9957	0.9936	
after extrapolation							
10^{-6}	8.6094(-004)	2.4311(-004)	6.4230(-005)	1.6260(-005)	3.8500(-006)	1.0000(-006)	5.4000(-007)
R_ε^N	1.8243	1.9203	1.9819	2.0784	1.9449	0.8890	
10^{-7}	8.6135(-004)	2.4346(-004)	6.4580(-005)	1.6630(-005)	4.2200(-006)	1.0400(-006)	2.5000(-007)
R_ε^N	1.8229	1.9145	1.9573	1.9785	2.0207	2.0566	
10^{-8}	8.6140(-004)	2.4348(-004)	6.4600(-005)	1.6670(-005)	4.2400(-006)	1.0800(-006)	2.9000(-007)
R_ε^N	1.8229	1.9142	1.9543	1.9751	1.9730	1.8969	
10^{-9}	8.6139(-004)	2.4350(-004)	6.45900(-005)	1.6670(-005)	4.2500(-006)	1.0800(-006)	2.9000(-007)
R_ε^N	1.8227	1.9145	1.9541	1.9717	1.9764	1.8969	
10^{-10}	8.6139(-004)	2.4350(-004)	6.4610(-005)	1.6660(-005)	4.2400(-006)	1.0800(-006)	2.9000(-007)
R_ε^N	1.8227	1.9141	1.9554	1.9743	1.9730	1.8969	

We have implemented the proposed numerical scheme on four standard example Problems 1 to 4 for diverse values of $N = \{2^3, 2^4, \ldots, 2^9\}$ and $\varepsilon = \{10^{-6}, 10^{-7}, 10^{-8}, 10^{-9}\}$ with $\delta = 0.5\varepsilon$ and presented the computational results in Tables 1 to 4 in terms of MAPEs and ROCs before and after applying Richardson extrapolation procedure to it. One can easily observe that the

Table 2: MAPEs (E_ε^N) and ROCs (R_ε^N) for diverse values of N and ε of Problem 2 for $\delta = 0.5\varepsilon$

ε	$N = 2^3$	$N = 2^4$	$N = 2^5$	$N = 2^6$	$N = 2^7$	$N = 2^8$	$N = 2^9$
before extrapolation							
10^{-6}	8.1429(-002)	3.9447(-002)	2.0202(-002)	1.0197(-002)	5.1213(-003)	2.5675(-003)	1.2861(-003)
R_ε^N	1.0456	0.9654	0.9864	0.9936	0.9961	0.9974	
10^{-7}	8.1428(-002)	3.9445(-002)	2.0201(-002)	1.0195(-002)	5.1200(-003)	2.5663(-003)	1.2849(-003)
R_ε^N	1.0457	0.9654	0.9866	0.9936	0.9965	0.9980	
10^{-8}	8.1428(-002)	3.9445(-002)	2.0201(-002)	1.0195(-002)	5.1199(-003)	2.5662(-003)	1.2847(-003)
R_ε^N	1.0457	0.9654	0.9866	0.9937	0.9965	0.9982	
10^{-9}	8.1428(-002)	3.9445(-002)	2.0201(-002)	1.0195(-002)	5.1199(-003)	2.5662(-003)	1.2847(-003)
R_ε^N	1.0457	0.9654	0.9866	0.9937	0.9965	0.9982	
10^{-10}	8.1428(-002)	3.9445(-002)	2.0201(-002)	1.0195(-002)	5.1199(-003)	2.5662(-003)	1.2847(-003)
R_ε^N	1.0457	0.9654	0.9866	0.9937	0.9965	0.9982	
after extrapolation							
10^{-6}	5.5340(-003)	1.7500(-003)	4.8230(-004)	1.2711(-004)	3.3660(-005)	9.7000(-006)	3.6500(-006)
R_ε^N	1.6610	1.8594	1.9239	1.9170	1.7950	1.4101	
10^{-7}	5.5325(-003)	1.7485(-003)	4.8086(-004)	1.2567(-004)	3.2180(-005)	8.2700(-006)	2.1800(-006)
R_ε^N	1.6618	1.8624	1.9360	1.9654	1.9602	1.9236	
10^{-8}	5.5323(-003)	1.7484(-003)	4.8070(-004)	1.2552(-004)	3.2030(-005)	8.1200(-006)	2.0500(-006)
R_ε^N	1.6618	1.8628	1.9372	1.9704	1.9799	1.9859	
10^{-9}	5.5323(-003)	1.7484(-003)	4.8070(-004)	1.2549(-004)	3.2030(-005)	8.1100(-006)	2.0200(-006)
R_ε^N	1.6618	1.8628	1.9376	1.9701	1.9816	2.0053	
10^{-10}	5.5323(-003)	1.7484(-003)	4.8070(-004)	1.2549(-004)	3.2030(-005)	8.0900(-006)	2.0300(-006)
R_ε^N	1.6618	1.8628	1.9376	1.9701	1.9852	1.9947	

application of Richardson extrapolation to the the solution of the original scheme improves the accuracy of the solution in such a way that the ROC of the proposed scheme is improving from 1 to 2. Furthermore, a simple comparison of the computational results presented in the Tables 5, 6, 7, and 8 with the results obtained in [60, 3, 58, 41] clearly reveal that the proposed scheme with Richardson extrapolation is capable of producing highly accurate and uniformly convergent results for all the values of $1/N \gg \varepsilon$, where $\varepsilon \leq 10^{-6}$. To examine the effect of the small delay (δ) on the solution behavior of the example Problems 1 to 4, we plotted the graphs of the obtained solution in Figures 1–8 for $N = 100$ and diverse values of $\delta = \{0.0\varepsilon, 0.3\varepsilon, 0.6\varepsilon, 0.9\varepsilon\}$ and $\varepsilon = \{10^{-1}, 10^{-2}\}$. These figures reveal that the thickness of the boundary layer decreases and form strong boundary layers when δ increases with fixed N and ε. For more clarity, in Figures

Table 3: MAPEs (E_ε^N) and ROCs (R_ε^N) for diverse values of N and ε of Problem 3 for $\delta = 0.5\varepsilon$

ε	$N = 2^3$	$N = 2^4$	$N = 2^5$	$N = 2^6$	$N = 2^7$	$N = 2^8$	$N = 2^9$
before extrapolation							
10^{-6}	2.4316(-002)	1.1480(-002)	5.5608(-003)	2.7345(-003)	1.3557(-003)	6.7510(-004)	3.3700(-004)
R_ε^N	1.0828	1.0458	1.0240	1.0122	1.0059	1.0024	
10^{-7}	2.4315(-002)	1.1479(-002)	5.5605(-003)	2.7342(-003)	1.3554(-003)	6.7480(-004)	3.3670(-004)
R_ε^N	1.0828	1.0457	1.0241	1.0124	1.0062	1.0030	
10^{-8}	2.4315(-002)	1.1479(-002)	5.5604(-003)	2.7342(-003)	1.3554(-003)	6.7480(-004)	3.3670(-004)
R_ε^N	1.0828	1.0457	1.0241	1.0124	1.0062	1.0030	
10^{-9}	2.4315(-002)	1.1479(-002)	5.5604(-003)	2.7342(-003)	1.3554(-003)	6.7470(-004)	3.3670(-004)
R_ε^N	1.0828	1.0457	1.0241	1.0124	1.0064	1.0028	
10^{-10}	2.4315(-002)	1.1479(-002)	5.5604(-003)	2.7341(-003)	1.3554(-003)	6.7470(-004)	3.3670(-004)
R_ε^N	1.0828	1.0457	1.0241	1.0123	1.0064	1.0028	
after extrapolation							
10^{-6}	1.3570(-003)	3.5830(-004)	9.2300(-005)	2.3500(-005)	6.0000(-006)	1.6000(-006)	5.0000(-007)
R_ε^N	1.9212	1.9568	1.9737	1.9696	1.9069	1.6781	
10^{-7}	1.3572(-003)	3.5840(-004)	9.2300(-005)	2.3600(-005)	6.0000(-006)	1.6000(-006)	5.0000(-007)
R_ε^N	1.9210	1.9572	1.9675	1.9758	1.9069	1.6781	
10^{-8}	1.3569(-003)	3.5840(-004)	9.2200(-005)	2.3600(-005)	6.0000(-006)	1.6000(-006)	5.0000(-007)
R_ε^N	1.9207	1.9587	1.9660	1.9758	1.9069	1.6781	
10^{-9}	1.3569(-003)	3.5840(-004)	9.2200(-005)	2.3600(-005)	6.0000(-006)	1.6000(-006)	5.0000(-007)
R_ε^N	1.9207	1.9587	1.9660	1.9758	1.9069	1.6781	
10^{-10}	1.3569(-003)	3.5840(-004)	9.2200(-005)	2.3300(-005)	6.0000(-006)	1.6000(-006)	5.0000(-007)
R_ε^N	1.9207	1.9587	1.9844	1.9573	1.9069	1.6781	

9–12, we have plotted the log-log plots for MAPE vs N (after extrapolation) for Problem 1 to 4 for various values of ε tending to zero. Through these figures, we easily observe that despite of increasing the value of N, for $\varepsilon = 10^{-6}$, the MAPE increases after certain value of N. Thus the method is capable of producing highly accurate and uniformly convergent results for all the values of $(1/N) \gg \varepsilon$ where $\varepsilon \leq 10^{-6}$.

8 Conclusion

A new exponentially fitted numerical scheme is addressed to approximate the solution of a class of SPDDEs having delay terms in the convection and reaction terms. Taylor's series expansion procedure has been used to approximate the terms containing the delay argument (δ). To increase the accuracy of the solution and the ROC of the scheme from 1 to 2, Richardson ex-

Table 4: MAPEs (E_ε^N) and ROCs (R_ε^N) for diverse values of N and ε of Problem 4 for $\delta = 0.5\varepsilon$

ε	$N=2^3$	$N=2^4$	$N=2^5$	$N=2^6$	$N=2^7$	$N=2^8$	$N=2^9$
before extrapolation							
10^{-6}	1.9855(-002)	1.0658(-002)	5.5309(-003)	2.8184(-003)	1.4226(-003)	7.1450(-004)	3.5787(-004)
R_ε^N	0.8976	0.9464	0.9726	0.9863	0.9935	0.9975	
10^{-7}	1.9856(-002)	1.0659(-002)	5.5314(-003)	2.8189(-003)	1.4231(-003)	7.1497(-004)	3.5833(-004)
R_ε^N	0.8975	0.9464	0.9725	0.9861	0.9931	0.9966	
10^{-8}	1.9856(-002)	1.0659(-002)	5.5315(-003)	2.8189(-003)	1.4231(-003)	7.1502(-004)	3.5838(-004)
R_ε^N	0.8975	0.9463	0.9725	0.9861	0.9930	0.9965	
10^{-9}	1.9856(-002)	1.0659(-002)	5.5315(-003)	2.8189(-003)	1.4231(-003)	7.1502(-004)	3.5838(-004)
R_ε^N	0.8975	0.9463	0.9725	0.9861	0.9930	0.9965	
10^{-10}	1.9856(-002)	1.0659(-002)	5.5315(-003)	2.8189(-003)	1.4231(-003)	7.1502(-004)	3.5838(-004)
R_ε^N	0.8975	0.9463	0.9725	0.9861	0.9930	0.9965	
after extrapolation							
10^{-6}	1.5751(-003)	4.4038(-004)	1.1714(-004)	2.9860(-005)	7.2300(-006)	1.4900(-006)	2.6000(-007)
R_ε^N	1.8386	1.9105	1.9719	2.0461	2.2787	2.5187	
10^{-7}	1.5756(-003)	4.4083(-004)	1.1756(-004)	3.0310(-005)	7.6700(-006)	1.9000(-006)	4.6000(-007)
R_ε^N	1.8376	1.9068	1.9555	1.9825	2.0132	2.0463	
10^{-8}	1.5756(-003)	4.4089(-004)	1.1761(-004)	3.0340(-005)	7.7100(-006)	1.9500(-006)	5.0000(-007)
R_ε^N	1.8374	1.9064	1.9547	1.9764	1.9833	1.9635	
10^{-9}	1.5757(-003)	4.4087(-004)	1.1760(-004)	3.0360(-005)	7.7300(-006)	1.9500(-006)	5.1000(-007)
R_ε^N	1.8376	1.9065	1.9536	1.9736	1.9870	1.9349	
10^{-10}	1.5756(-003)	4.4088(-004)	1.1763(-004)	3.0350(-005)	7.7000(-006)	1.9700(-006)	5.1000(-007)
R_ε^N	1.8374	1.9061	1.9545	1.9788	1.9667	1.9496	

Table 5: Comparison of MAPEs (E_ε^N) for diverse values of N and ε of Problem 1

ε	$N=2^5$	$N=2^6$	$N=2^7$	$N=2^8$	$N=2^9$	$N=2^{10}$
2^{-20}	6.4250(-005)	1.6310(-005)	3.8700(-006)	9.8000(-007)	5.3000(-007)	4.2000(-007)
2^{-24}	6.4580(-005)	1.6650(-005)	4.2200(-006)	1.0600(-006)	2.7000(-007)	8.0000(-008)
2^{-28}	6.4620(-005)	1.6640(-005)	4.2500(-006)	1.0800(-006)	2.9000(-007)	9.0000(-008)
2^{-32}	6.4610(-005)	1.6640(-005)	4.2500(-006)	1.0800(-006)	2.9000(-007)	9.0000(-008)
result in [60]						
2^{-20}	4.7320(-003)	2.4804(-003)	1.2705(-003)	6.4304(-004)	3.2349(-004)	1.6223(-004)
2^{-24}	4.7320(-003)	2.4804(-003)	1.2705(-003)	6.4307(-004)	3.2352(-004)	1.6226(-004)
2^{-28}	4.7320(-003)	2.4804(-003)	1.2705(-003)	6.4307(-004)	3.2352(-004)	1.6226(-004)
2^{-32}	4.7320(-003)	2.4804(-003)	1.2705(-003)	6.4307(-004)	3.2352(-004)	1.6226(-004)
result in [3]						
2^{-20}	0.12360(-001)	0.62211(-002)	0.31206(-002)	0.15628(-002)	0.78203(-003)	0.39117(-003)
2^{-24}	0.12360(-001)	0.62211(-002)	0.31206(-002)	0.15628(-002)	0.78203(-003)	0.39117(-003)
2^{-28}	0.12360(-001)	0.62211(-002)	0.31206(-002)	0.15628(-002)	0.78203(-003)	0.39117(-003)
2^{-32}	0.12360(-001)	0.62211(-002)	0.31206(-002)	0.15628(-002)	0.78203(-003)	0.39117(-003)

trapolation technique is applied. Numerical experiments are performed to show the applicability of the proposed method. Convergence and stability are also examined. Numerical results are noted in tabular form in terms of MAPEs and the ROCs before and after applying the Richard-

Table 6: Comparison of MAPEs (E_ε^N) for diverse values of N and ε of Problem 2

ε	$N=2^5$	$N=2^6$	$N=2^7$	$N=2^8$	$N=2^9$	$N=2^{10}$
10^{-10}	4.8070(-004)	1.2549(-004)	3.2030(-005)	8.0900(-006)	2.0300(-006)	5.2000(-007)
10^{-12}	4.8070(-004)	1.2549(-004)	3.2030(-005)	8.0900(-006)	2.0300(-006)	5.2000(-007)
10^{-15}	4.8070(-004)	1.2549(-004)	3.2030(-005)	8.0900(-006)	2.0300(-006)	5.2000(-007)
10^{-20}	4.8070(-004)	1.2549(-004)	3.2030(-005)	8.0900(-006)	2.0300(-006)	5.2000(-007)
result in [60]						
10^{-10}	7.9338(-003)	4.0004(-003)	2.0070(-003)	1.0060(-003)	5.0411(-004)	2.5064(-004)
10^{-12}	7.9338(-003)	4.0004(-003)	2.0070(-003)	1.0060(-003)	5.0411(-004)	2.5064(-004)
10^{-15}	7.9338(-003)	4.0004(-003)	2.0070(-003)	1.0060(-003)	5.0411(-004)	2.5064(-004)
10^{-20}	7.9338(-003)	4.0004(-003)	2.0070(-003)	1.0060(-003)	5.0411(-004)	2.5064(-004)

Figure 1: Solution graph for Problem 1 for $N=100$, $\varepsilon=\frac{1}{10}$ and various values of δ of $o(\varepsilon)$

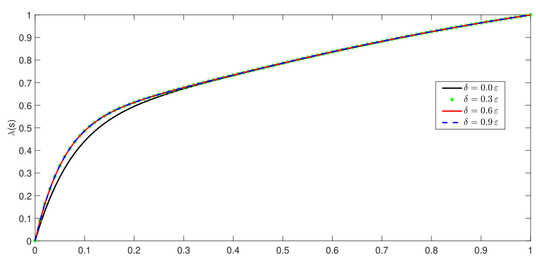

Figure 2: Solution graph for Problem 1 for $N=100$, $\varepsilon=\frac{1}{100}$ and various values of δ of $o(\varepsilon)$

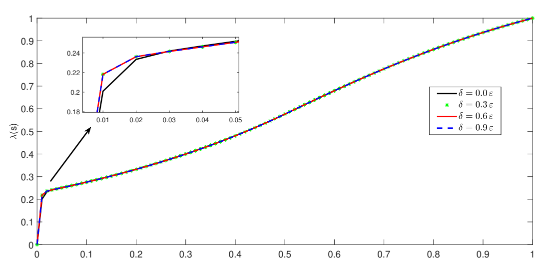

son extrapolation. The results are compared to the results in [60, 3, 58, 41]. The method is successfully achieving quadratic order convergence with higher accuracy. Solution graphs for the considered example problems produced by the proposed numerical technique are plotted for

Table 7: Comparison of MAPEs (E_ε^N) for diverse values of N and ε of Problem 3

ε	$N=2^5$	$N=2^6$	$N=2^7$	$N=2^8$	$N=2^9$	$N=2^{10}$
10^{-9}	9.2200(-005)	2.3600(-005)	6.0000(-006)	1.6000(-006)	5.0000(-007)	3.0000(-007)
10^{-10}	9.2200(-005)	2.3300(-005)	6.0000(-006)	1.6000(-006)	5.0000(-007)	3.0000(-007)
10^{-11}	9.2200(-005)	2.3300(-005)	6.0000(-006)	1.6000(-006)	5.0000(-007)	3.0000(-007)
10^{-12}	9.2200(-005)	2.3300(-005)	6.0000(-006)	1.6000(-006)	5.0000(-007)	3.0000(-007)
10^{-13}	9.2200(-005)	2.3300(-005)	6.0000(-006)	1.6000(-006)	5.0000(-007)	3.0000(-007)
result in [60]						
10^{-9}	4.4394(-003)	2.3357(-003)	1.1972(-003)	6.0599(-003)	3.0464(-004)	1.5287(-004)
10^{-10}	4.4394(-003)	2.3357(-003)	1.1972(-003)	6.0599(-003)	3.0464(-004)	1.5287(-004)
10^{-11}	4.4394(-003)	2.3357(-003)	1.1972(-003)	6.0599(-003)	3.0464(-004)	1.5287(-004)
10^{-12}	4.4394(-003)	2.3357(-003)	1.1972(-003)	6.0599(-003)	3.0464(-004)	1.5287(-004)
10^{-13}	4.4394(-003)	2.3357(-003)	1.1972(-003)	6.0599(-003)	3.0464(-004)	1.5287(-004)
result in [3]						
10^{-9}	4.8030(-003)	2.5439(-003)	1.3085(-003)	6.6353(-004)	3.3410(-004)	1.6763(-004)
10^{-10}	4.8030(-003)	2.5439(-003)	1.3085(-003)	6.6353(-004)	3.3410(-004)	1.6763(-004)
10^{-11}	4.8030(-003)	2.5439(-003)	1.3085(-003)	6.6353(-004)	3.3410(-004)	1.6763(-004)
10^{-12}	4.8030(-003)	2.5439(-003)	1.3085(-003)	6.6353(-004)	3.3410(-004)	1.6763(-004)
10^{-13}	4.8030(-003)	2.5439(-003)	1.3085(-003)	6.6353(-004)	3.3410(-004)	1.6763(-004)
result in [58]						
10^{-9}	0.066(-001)	0.042(-001)	0.023(-001)	0.012(-001)	0.064(-002)	0.032(-002)
10^{-10}	0.066(-001)	0.042(-001)	0.023(-001)	0.012(-001)	0.064(-002)	0.032(-002)
10^{-11}	0.066(-001)	0.042(-001)	0.023(-001)	0.012(-001)	0.064(-002)	0.032(-002)
10^{-12}	0.066(-001)	0.042(-001)	0.023(-001)	0.012(-001)	0.064(-002)	0.032(-002)
10^{-13}	0.066(-001)	0.042(-001)	0.023(-001)	0.012(-001)	0.064(-002)	0.032(-002)
result in [41]						
10^{-9}	0.18(-001)	0.93(-002)	0.47(-002)	0.24(-002)	0.12(-002)	0.59(-003)
10^{-10}	0.18(-001)	0.93(-002)	0.47(-002)	0.24(-002)	0.12(-002)	0.59(-003)
10^{-11}	0.18(-001)	0.93(-002)	0.47(-002)	0.24(-002)	0.12(-002)	0.59(-003)
10^{-12}	0.18(-001)	0.93(-002)	0.47(-002)	0.24(-002)	0.12(-002)	0.59(-003)
10^{-13}	0.18(-001)	0.93(-002)	0.47(-002)	0.24(-002)	0.12(-002)	0.59(-003)

Table 8: Comparison of MAPEs (E_ε^N) for diverse values of N and ε of Problem 4

ε	$N=2^4$	$N=2^5$	$N=2^6$	$N=2^7$	$N=2^8$	$N=2^9$
10^{-9}	4.4087(-004)	1.1760(-004)	3.0360(-005)	7.7300(-006)	1.9500(-006)	5.1000(-007)
10^{-10}	4.4088(-004)	1.1763(-004)	3.0350(-005)	7.7000(-006)	1.9700(-006)	5.1000(-007)
10^{-11}	4.4088(-004)	1.1763(-004)	3.0350(-005)	7.7200(-006)	1.9700(-006)	5.1000(-007)
10^{-12}	4.4088(-004)	1.1763(-004)	3.0350(-005)	7.7200(-006)	1.9700(-006)	5.1000(-007)
10^{-13}	4.4088(-004)	1.1763(-004)	3.0350(-005)	7.7200(-006)	1.9700(-006)	5.1000(-007)
result in [58]						
10^{-9}	0.40(-002)	0.20(-002)	0.10(-002)	0.51(-003)	0.26(-003)	0.13(-003)
10^{-10}	0.40(-002)	0.20(-002)	0.10(-002)	0.51(-003)	0.26(-003)	0.13(-003)
10^{-11}	0.40(-002)	0.20(-002)	0.10(-002)	0.51(-003)	0.26(-003)	0.13(-003)
10^{-12}	0.40(-002)	0.20(-002)	0.10(-002)	0.51(-003)	0.26(-003)	0.13(-003)
10^{-13}	0.40(-002)	0.20(-002)	0.10(-002)	0.51(-003)	0.26(-003)	0.13(-003)
result in [41]						
10^{-9}	0.11(-001)	0.57(-002)	0.29(-002)	0.14(-002)	0.72(-003)	0.36(-003)
10^{-10}	0.11(-001)	0.57(-002)	0.29(-002)	0.14(-002)	0.72(-003)	0.36(-003)
10^{-11}	0.11(-001)	0.57(-002)	0.29(-002)	0.14(-002)	0.72(-003)	0.36(-003)
10^{-12}	0.11(-001)	0.57(-002)	0.29(-002)	0.14(-002)	0.72(-003)	0.36(-003)
10^{-13}	0.11(-001)	0.57(-002)	0.29(-002)	0.14(-002)	0.72(-003)	0.36(-003)

Figure 3: Solution graph for Problem 2 for $N = 100$, $\varepsilon = \frac{1}{10}$ and various values of δ of $o(\varepsilon)$

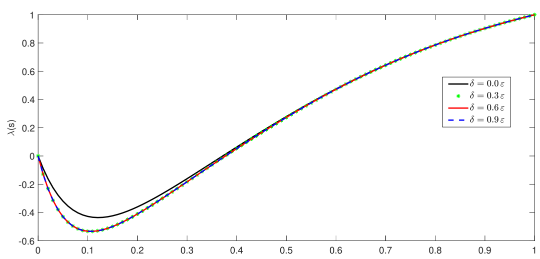

Figure 4: Solution graph for Problem 2 for $N = 100$, $\varepsilon = \frac{1}{100}$ and various values of δ of $o(\varepsilon)$

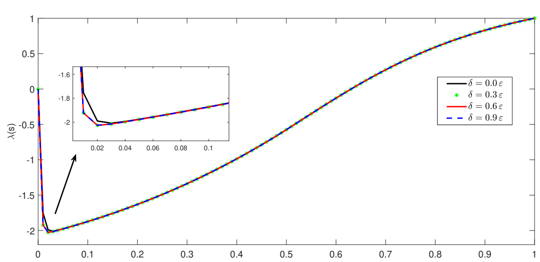

Figure 5: Solution graph for Problem 3 for $N = 100$, $\varepsilon = \frac{1}{10}$ and various values of δ of $o(\varepsilon)$

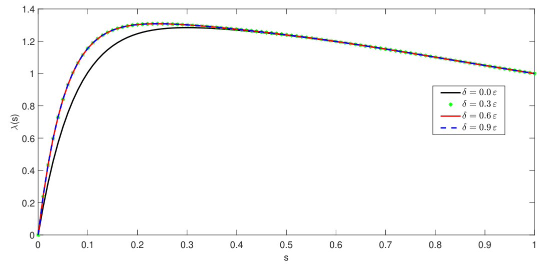

Figure 6: Solution graph for Problem 3 for $N = 100$, $\varepsilon = \frac{1}{100}$ and various values of δ of $o(\varepsilon)$

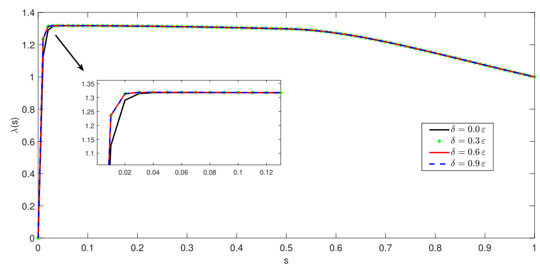

Figure 7: Solution graph for Problem 4 for $N = 100$, $\varepsilon = \frac{1}{10}$ and various values of δ of $o(\varepsilon)$

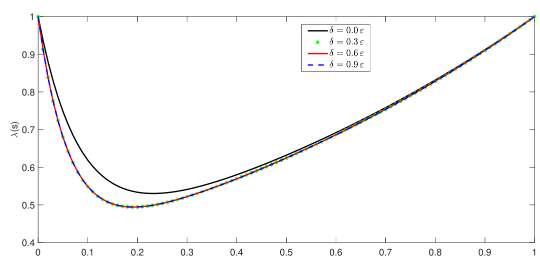

Figure 8: Solution graph for Problem 4 for $N = 100$, $\varepsilon = \frac{1}{100}$ and various values of δ of $o(\varepsilon)$

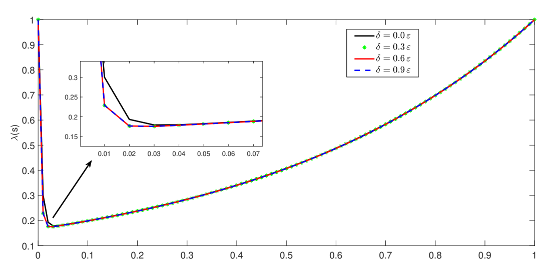

Figure 9: Log-log plot for MAPE vs N for Problem 1 for various values of ε

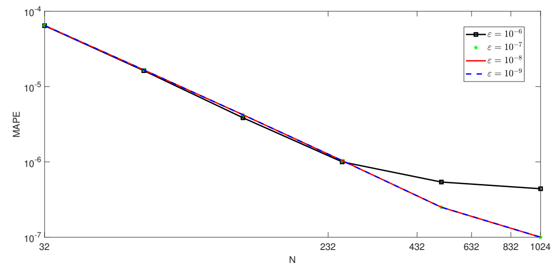

Figure 10: Log-log plot for MAPE vs N for Problem 2 for various values of ε

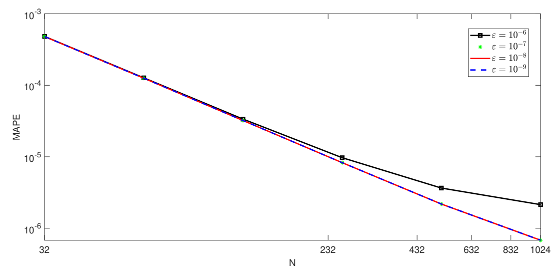

Figure 11: Log-log plot for MAPE vs N for Problem 2 for various values of ε

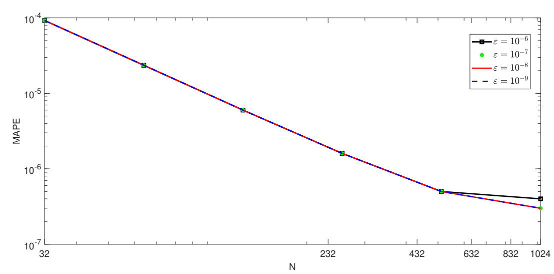

Figure 12: Log-log plot for MAPE vs N for Problem 4 for various values of ε

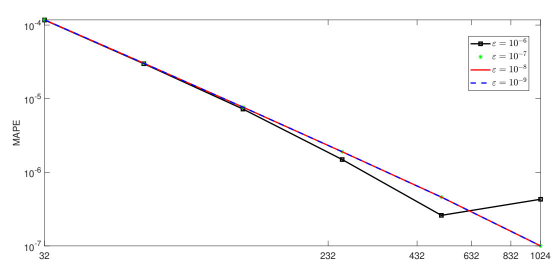

$N = 100$ and different values of δ and ε. These graphs show that as the delay argument (δ) increases and $\varepsilon \to 0$, the thickness of the boundary layer decreases. For more clarity, in Figures 9, 10, 11, and 12, we have plotted the log-log plots for MAPE vs N (after extrapolation) for the considered Problems 1 to 4 for various values of ε. Through these figures, we easily observe that despite increasing the value of N, for $\varepsilon = 10^{-6}$, the MAPE increases after certain value of N. Thus the method is capable of producing highly accurate and uniformly convergent results for all the values of $(1/N) \gg \varepsilon$ where $\varepsilon \leq 10^{-6}$. Novelty of the proposed method is associated with the improvement in the accuracy of the solutions in such a way that the ROC increases from 1 to 2, when the Richardson extrapolation procedure is applied. For some methods/schemes, the accuracy of the solutions obtained improves, but the ROC does not when the Richardson extrapolation procedure is applied to it [50, 51].

Acknowledgements

Authors are grateful to the anonymous referees and editor for their constructive comments.

Funding

This research received no external funding.

Conflicts of Interest

The authors declare no conflicts of interest.

References

[1] Alam, M.J., Prasad, H.S. and Ranjan, R. *A novel fitted method for a class of singularly perturbed differential-difference equations with small delay exhibiting twin layer or oscillatory behavior*, Comput. Math. Math. Phys. 63(12) (2023), 2528–2550.

[2] Andreev, V.F. and Popov, A.M. *Using Richardson's method to construct high-order accurate adaptive grids*, Comput. Math. Model. 10(3) (1999), 227–238.

[3] Angasu, M.A., Duressa, G.F. and Woldaregay, M.M. *Exponentially fitted numerical scheme for singularly perturbed differential equations involving small delays*, J. Appl. Math. Inform. 39(3-4) (2021), 419–435.

[4] Bala, S. and Govindarao, L. and Das, A. and Majumdar, A. *Numerical scheme for partial differential equations involving small diffusion term with non-local boundary conditions*, J. Appl. Math. Comput. 69(6) (2023), 4307–4331.

[5] Balachandran, B. and Kalmár-Nagy, T. and Gilsinn, D.E. *Delay differential equations*, Springer, New York, 2009.

[6] Banasiak, J. and Lachowicz, M. *Methods of small parameter in mathematical biology*, Springer, New York, 2014.

[7] Bawa, R. K. *Spline based computational technique for linear singularly perturbed boundary value problems*, Appl. Math. Comput., 167(1) (2005), 225–236.

[8] Bellen, A. and Zennaro, M. *Numerical methods for delay differential equations*, Springer, Cham, Switzerland, 2013.

[9] Bellman, R. E. and Kalaba, R. E. *Quasilinearization and nonlinear boundary-value problems*, American Elsevier Publishing Company, New York, 1965.

[10] Bender, C. M. and Orszag, S. A. *Advanced mathematical methods for scientists and engineers I: Asymptotic methods and perturbation theory*, Springer Science & Business Media, New York, 2013.

[11] Cooke, K. L. *Differential–difference equations*, in: International Symposium on Nonlinear Differential Equations and Nonlinear Mechanics, Elsevier, 1963, 155–171.

[12] Das, A., Govindarao, L. and Mohapatra, J. *A second-order weighted monotone numerical scheme for time-delayed parabolic initial-boundary-value problem involving a small parameter*, Int. J. Math. Model. Numer. Optim. 12(3) (2022), 233–251.

[13] Das, A. and Natesan, S. *Second-order uniformly convergent numerical method for singularly perturbed delay parabolic partial differential equations*, Int. J. Comput. Math. 95(3) (2018), 490–510.

[14] Das, P. *Comparison of a priori and a posteriori meshes for singularly perturbed nonlinear parameterized problems*, J. Comput. Appl. Math. 290 (2015), 16–25.

[15] Das, P. *A higher order difference method for singularly perturbed parabolic partial differential equations*, J. Difference Equ. Appl. 24(3) (2018), 452–477.

[16] Das, P. *An a posteriori based convergence analysis for a nonlinear singularly perturbed system of delay differential equations on an adaptive mesh*, Numer. Algorithms 81(2) (2019), 465–487.

[17] Das, P. and Natesan, S. *A uniformly convergent hybrid scheme for singularly perturbed system of reaction-diffusion Robin type boundary-value problems*, J. Appl. Math. Comput. 41 (2013), 447–471.

[18] Doolan, E.P. and Miller, J.J.H. and Schilders, W.H.A. *Uniform numerical methods for problems with initial and boundary layers*, Boole Press, Dublin, 1980.

[19] Driver, R.D. *Ordinary and delay differential equations*, Springer, New York, 1977.

[20] Duressa, G.F., Daba, I.T. and Deressa, C.T. *A systematic review on the solution methodology of singularly perturbed differential difference equations*, Mathematics 11(5) (2023), 1108.

[21] Duressa, G.F. and Debela, H.G. *Numerical solution of singularly perturbed differential difference equations with mixed parameters*, J. Math. Model. 9(4) (2021), 691–705.

[22] Fouque, J.-P., Papanicolaou, G. and Sircar, R. and Solna, K. *Singular perturbations in option pricing*, SIAM J. Appl. Math. 63(5) (2003), 1648–1665.

[23] Hek, G. *Geometric singular perturbation theory in biological practice*, J. Math. Biol. 60(3) (2010), 347–386.

[24] Hutchinson, G.E. *Circular causal systems in ecology*, Ann. N. Y. Acad. Sci. 50(4) (1948), 221–246.

[25] Joy, D. and Kumar, S.D. *Liouville–Green transformation technique to solve singularly perturbed delay differential equations of reaction diffusion type*, Math. Methods Appl. Sci. 48(10) (2025), 10314–10331.

[26] Joy, D., Kumar, S.D. and Rihan, F.A. *Advancing numerical solutions for a system of singularly perturbed delay differential equations at linear rate*, Bound. Value Probl. 2025(1) (2025), 15.

[27] Joy, D. and Regal, A.M. *Tension spline approach to singularly perturbed delay differential equations involving large delay*, Gulf J. Math. 15(2) (2023), 166–174.

[28] Kadalbajoo, M.K. and Gupta, V. *A brief survey on numerical methods for solving singularly perturbed problems*, Appl. Math. Comput. 217(8) (2010), 3641–3716.

[29] Kadalbajoo, M.K. and Patidar, K.C. *Singularly perturbed problems in partial differential equations: A survey*, Appl. Math. Comput. 134(2–3) (2003), 371–429.

[30] Kadalbajoo, M.K. and Patidar, K.C. and Sharma, K.K. *ε-uniformly convergent fitted methods for the numerical solution of the problems arising from singularly perturbed general DDEs*, Appl. Math. Comput. 182(1) (2006), 119–139.

[31] Kadalbajoo, M.K. and Reddy, Y.N. *Numerical solution of singular perturbation problems via deviating arguments*, Appl. Math. Comput. 21(3) (1987), 221–232.

[32] Kadalbajoo, M.K. and Yadaw, A.S. and Kumar, D. *Comparative study of singularly perturbed two-point BVPs via: Fitted-mesh finite difference method, B-spline collocation method and finite element method*, Appl. Math. Comput. 204(2) (2008), 713–725.

[33] Kaur, J. and Kaur, B. *A Review on singularly perturbed problems*, IJRAR (2023).

[34] Kuang, Y. *Delay differential equations*, Academic Press, New York, 1993.

[35] Kumar, D. and Kadalbajoo, M.K. *Numerical treatment of singularly perturbed delay differential equations using B-spline collocation method on Shishkin mesh*, J. Numer. Anal. Ind. Appl. Math. 7(3–4) (2012), 73–90.

[36] Kumar, M. and Singh, P. and Mishra, H.K. *A recent survey on computational techniques for solving singularly perturbed boundary value problems*, Int. J. Comput. Math. 84(10) (2007), 1439–1463.

[37] Lakshmikantham, V. and Wen, L. and Zhang, B. *Theory of differential equations with unbounded delay*, Springer, New York, 2013.

[38] Lange, C.G. and Miura, R.M. *Singular perturbation analysis of boundary value problems for differential-difference equations*, SIAM J. Appl. Math. 42(3) (1982), 502–531.

[39] Lange, C.G. and Miura, R.M. *Singular perturbation analysis of boundary-value problems for differential-difference equations. II. Rapid oscillations and resonances*, SIAM J. Appl. Math. 45(5) (1985), 687–707.

[40] Lange, C.G. and Miura, R.M. *Singular perturbation analysis of boundary-value problems for differential-difference equations. III. Turning point problems*, SIAM J. Appl. Math. 45(5) (1985), 708–734.

[41] Lange, C.G. and Miura, R.M. *Singular perturbation analysis of boundary-value problems for differential-difference equations. V. small shifts with layer behavior*, SIAM J. Appl. Math. 54(1) (1994), 249–272.

[42] Lange, C.G. and Miura, R.M. *Singular perturbation analysis of boundary-value problems for differential-difference equations. VI. small shifts with rapid oscillations*, SIAM J. Appl. Math. 54(1) (1994), 273–283.

[43] Linß, T. *An upwind difference scheme on a novel Shishkin-type mesh for a linear convection–diffusion problem*, J. Comput. Appl. Math. 110(1) (1999), 93–104.

[44] Linß, T. *Solution decompositions for linear convection-diffusion problems*, Z. Anal. Anwend. 21(1) (2002), 209–214.

[45] Linß, T. and Stynes, M. *A hybrid difference scheme on a Shishkin mesh for linear convection–diffusion problems*, Appl. Numer. Math. 31(3) (1999), 255–270.

[46] Longtin, A. and Milton, J.G. *Complex oscillations in the human pupil light reflex with mixed and delayed feedback*, Math. Biosci. 90(1–2) (1988), 183–199.

[47] Miller, J.J.H. *Singular perturbation problems in chemical physics: Analytic and computational methods*, Wiley, New York, 1997.

[48] Miller, J.J.H. and O'Riordan, E. and Shishkin, G.I. *Fitted numerical methods for singular perturbation problems*, World Scientific, Singapore, 1996.

[49] Mukherjee, K. and Natesan, S. *Richardson extrapolation technique for singularly perturbed parabolic convection–diffusion problems*, Computing 92(1) (2011), 1–32.

[50] Munyakazi, J.B. and Patidar, K.C. *Limitations of Richardson's extrapolation for a high-order fitted mesh method for self-adjoint singularly perturbed problems*, J. Appl. Math. Comput. 32(1) (2010), 219–236.

[51] Munyakazi, J.B. and Patidar, K.C. *Performance of Richardson extrapolation on some numerical methods for a singularly perturbed turning point problem whose solution has boundary layers*, J. Korean Math. Soc. 51(4) (2014), 679–702.

[52] Mushahary, P. and Sahu, S.R. and Mohapatra, J. *A parameter uniform numerical scheme for singularly perturbed differential-difference equations with mixed shifts*, J. Appl. Comput. Mech. 6(2) (2020), 344–356.

[53] Norkin, S.B. *Differential equations of the second-order with retarded argument: some problems of the theory of vibrations of systems with retardation*, American Mathematical Society 1972.

[54] Norkin, S.B. *Introduction to the theory and application of differential equations with deviating arguments*, (Vol. 105), Academic Press, 1973.

[55] O'Malley Jr., R.E. *Introduction to singular perturbations*, J. Fluid Mech. 1974.

[56] O'Malley, Jr. R.E. *Singular perturbation methods for ordinary differential equations*, Springer-Verlag, Berlin, 1991.

[57] O'Malley Jr., R.E., Kevorkian J. and Cole, J.D. *Perturbation methods in applied mathematics, and Ali Hasan Nayfeh, Introduction to perturbation techniques*, J. Fluid Mech. 71(4) (1982), 827–828.

[58] Phaneendra, K. and Lalu, M. *Numerical solution of singularly perturbed delay differential equations using Gaussian quadrature method*, J. Phys. Conf. Ser. 1344(1) (2019), 012013.

[59] Prasad, H.S. and Reddy, Y.N. *Numerical solution of singularly perturbed differential-difference equations with small shifts of mixed type by differential quadrature method*, Am. J. Comput. Appl. Math. 2(1) (2012), 46–52.

[60] Ranjan, R. *A novel fitted spline method for the numerical treatment of singularly perturbed differential equations having small delays*, J. Appl. Math. Comput. 69(6) (2023), 4645–4664.

[61] Ranjan, R. and Prasad, H.S. *A novel exponentially fitted finite difference method for a class of 2nd order singularly perturbed boundary value problems with a simple turning point exhibiting twin boundary layers*, J. Ambient Intell. Humaniz. Comput. 13(9) (2022), 4207–4221.

[62] Ranjan, R., Prasad, H.S. and Kiltu, G.G. *A novel fitted three-term method for the numerical treatment of singularly perturbed differential–difference equations*, Mediterr. J. Math. 21(2) (2024), 53.

[63] Raza, A., Khan, A., and Sharma, P. and Ahmad, K. *Solution of singularly perturbed differential difference equations and convection delayed dominated diffusion equations using Haar wavelet*, Math. Sci. 15 (2021), 123–136.

[64] Reddy, Y.N. and Reddy, K.A. *Numerical integration method for general singularly perturbed two-point boundary value problems*, Appl. Math. Comput. 133(2–3) (2002), 351–373.

[65] Regal, A.M. and Kumar, S.D. *Non-polynomial spline method for singularly perturbed differential difference equations with delay and advance terms*, Bull. Karaganda Univ. Math. Ser. 118(2) (2025), 208–221.

[66] Regal, A.M. and Kumar, S.D. *Numerical approximation for singularly perturbed differential equations exhibiting significant positive shift arising in neuronal activity*, Appl. Math. Sci. Eng. 33(1) (2025), 2498414.

[67] Sharma, N. and Kaushik, A. *A uniformly convergent difference method for singularly perturbed parabolic partial differential equations with large delay and integral boundary condition*, J. Appl. Math. Comput. 69(1) (2023), 1071–1093.

[68] Shishkin, G.I. and Shishkina, L.P. *The Richardson extrapolation technique for quasilinear parabolic singularly perturbed convection–diffusion equations*, J. Phys. Conf. Ser. 55(1) (2006), 203–209.

[69] Stein, R.B. *Some models of neuronal variability*, Biophys. J. 7(1) (1967), 37–68.

[70] Stynes, M. and Roos, H.-G. *The midpoint upwind scheme*, Appl. Numer. Math. 23(3) (1997), 361–374.

[71] Tian, H. *The exponential asymptotic stability of singularly perturbed delay differential equations with a bounded lag*, J. Math. Anal. Appl. 270(1) (2002), 143–149.

[72] Tuckwell, H.C. *On the first-exit time problem for temporally homogeneous Markov processes*, J. Appl. Probab. (1976), 39–48.

[73] Villasana, M. and Radunskaya, A. *A delay differential equation model for tumor growth*, J. Math. Biol. 47(3) (2003), 270–294.

[74] Wazewska-Czyzewska, M. and Lasota, A. *Mathematical models of the red cell system*, Mat. Stos. 6(1) (1976), 25–40.

[75] Woldaregay, M.M. *Solving singularly perturbed delay differential equations via fitted mesh and exact difference method*, Res. Math. 9(1) (2022), 2109301.

[76] Woldaregay, M.M. and Duressa, G.F. *Higher-order uniformly convergent numerical scheme for singularly perturbed differential difference equations with mixed small shifts*, Int. J. Differ. Equ. 2020(1) (2020), 6661592.

[77] Woldaregay, M.M. and Duressa, G.F. *Robust mid-point upwind scheme for singularly perturbed delay differential equations*, Comput. Appl. Math. 40(5) (2021), 178.

[78] Woldaregay, M.M. and Duressa, G.F. *Robust numerical scheme for solving singularly perturbed differential equations involving small delays*, Appl. Math. E-Notes, 21 (2021), 622–633.